International Journal of Heat and Mass Transfer 52 (2009) 4624–4634

Contents lists available at ScienceDirect

International Journal of Heat and Mass Transfer

journal homepage: www.elsevier.com/locate/ijhmt

Measurement and prediction of the rate of deposition of flocculated asphaltene particles from oil

M. Jamialahmadi [a], B. Soltani [b], H. Müller-Steinhagen [c,d,*], D. Rashtchian [b]

[a] University of Petroleum Industry, Ahwaz, Iran
[b] Department of Chemical and Petroleum Engineering, Sharif University, Tehran, Iran
[c] Institute for Technical Thermodynamics, German Aerospace Centre (DLR), Germany
[d] Institute for Thermodynamics and Thermal Engineering, University of Stuttgart, Pfaffenwaldring 6, 70550 Stuttgart, Germany

ARTICLE INFO

Article history:
Received 15 April 2008
Received in revised form 7 December 2008
Accepted 13 January 2009
Available online 4 May 2009

Keywords:
Oil production
Asphaltene precipitation
Deposition rates
Modeling

ABSTRACT

Asphaltene deposition is one of the unresolved problems in oil industries. Little information is available on the critical question of "how fast" the flocculated asphaltene particles deposit across the production wells from the flowing oil. In this study, the mechanisms of deposition of flocculated asphaltene particles from oil have been studied experimentally and theoretically under forced convective conditions using an accurate thermal approach. The effects of oil velocity, flocculated asphaltene concentration and temperature on the rate of asphaltene deposition are investigated. It is observed that during the first few weeks the deposition mechanism is dominant and the erosion of the deposit is almost negligible. The rate of asphaltene deposition increases with increasing flocculated asphaltene concentration and temperature while it decreases with increasing oil velocity. After clarification of the effects of operating parameters on the deposition process, the results of the experiments are used to develop a mechanistic model for the prediction of the rate of asphaltene deposit formation under forced convective conditions. The predictions of the suggested model for the deposition rate of asphaltene are compared with measured data. Quantitative and qualitative agreement between measured and predicted asphaltene deposition rates is good.

1. Introduction

Crude oil is a colloidal mixture consisting of various fractions of saturated hydrocarbons, aromatics, resins and asphaltenes (e.g. Mullins and Sheu [1]). Amongst these, asphaltene is viewed as the most polar and highest molecular weight fraction of the crude oil. The chemical structure of asphaltene has been the subject of many studies (e.g. Yen et al. [2], Speight [3], Yen [4]). These investigations reveal that asphaltenes are stabilized in oil by the resin molecules which act as peptizing agent for emulsifying asphaltene particles. Colloidal asphaltenes may be naturally or artificially precipitated from oil if the resin molecules are removed from the surface of the asphaltene particles. Resins are normally classified as the fraction of crude oil which is soluble in normal alkane solvents such as normal pentane while asphaltenes are soluble in aromatic solvents such as toluene and xylene (Burke et al. [5]). Asphaltenes have a brownish appearance and consist chemically of a mixture of polar aromatic and naphthenic molecules which contain heteroatoms of nitrogen, sulfur and oxygen. They are flocculated by normal alkanes including those with small carbon number such as propane (Andersen [6], Rassamdana et al. [7], Hu et al. [8]). The degree of resin removal from the surface of asphaltene particles depends strongly on the carbon number of the normal alkane solvents and increases with increasing carbon number (Hu et al. [8], Vazquez and Mansoori [9]). Deposition can also be enhanced by any chemical, mechanical or electrical processes which are able to depeptize colloidal particles and thus lead to flocculation and precipitation of asphaltene (Kokal et al. [10]).

Asphaltene deposition is a major unresolved problem in the oil industry which may occur during primary oil production and subsequent enhanced oil recovery methods. The existence of concentration gradients accompanied by pressure and temperature profiles across the reservoir formation, especially in the vicinity of the bottom hole of the production wells, in well tubing and in surface facilities affects the stability of colloidal asphaltene particles and provides favorable conditions for their deposition (e.g. Kabir and Jamaluddin [11], Kokal et al. [12]). Deposition of flocculated asphaltene particles can sometimes be so severe that it may limit or block well tubing, pumps and other production equipment and facilities. Due to asphaltene deposition, primary recovery from oil reservoirs in which the pressure has declined close to the bubble point pressure can present many operational problems and, therefore, severely limit the production rate. From reservoir

* Corresponding author. Address: Institute for Thermodynamics and Thermal Engineering, University of Stuttgart, Pfaffenwaldring 6, 70550 Stuttgart, Germany. Tel.: +49 71168563536; fax: +49 71168563533.
E-mail address: hms@itw.uni-stuttgart.de (H. Müller-Steinhagen).

0017-9310/$ - see front matter © 2009 Published by Elsevier Ltd.
doi:10.1016/j.ijheatmasstransfer.2009.01.049

Nomenclature

a and b	constants
A_p	cross-sectional area of the particle in flow direction, m^2
$A_0 - A_3$	constants
C	concentration, kg/m^3
C_D	drag coefficient
C_P	specific heat, J/kg K
D	tube diameter, m
d_p	particle diameter, m
D_{Diff}	diffusion coefficient, m^2/s
E_a	attachment activation energy, J/mole
f	Darcy friction factor
F_{adh}	adhesion force, N
F_{drag}	drag force, N
$k_{1,2}$	constants
k_t	transport coefficient, m/s
k_d	coefficient in eq. (35), m/s
$k_{d'}$	coefficient in eq. (36), m/s
k_B	Boltzmann constant = 1.38×10^{-23} J/K
L	length, m
m	mass of deposit per unit area, kg/m^2
$\dot{m}$	rate of deposition or removal, kg/m^2 s
Nu	Nusselt number
M	molecular weight of solvent, kg/kmol
Pr	Prandtl number
$\dot{q}$	heat flux, W/m^2
r	radius, m
R_A	thermal resistance of deposit, m^2 K/W
R_m	solvent to oil ratio, m^3/kg
R_v	solvent to oil ratio, m^3/m^3
Re	Reynolds number
s	distance between thermocouple location and heat transfer surface, m
Sc	Schmidt number
Sh	Sherwood number
S_p	sticking probability
S_0	constant
t	time, s
T	temperature, K
v	oil velocity, m/s
W	weight percent of asphaltene precipitation
Wt%	composition in weight percent
X and Y	scaling parameters, defined by Eq. (8)

Greek symbols

α	heat transfer coefficient, W/m^2 K
β	mass transfer coefficient, m/s
λ	thermal conductivity, W/m K
μ	oil viscosity, kg/ms
ρ	density, kg/m^3

Subscripts–superscripts

A	asphaltene
b	bulk
d	deposit
fc	forced convection
o	oil or outside
r	removal
s	surface
t	at time t
th	thermocouple
$turb$	turbulent
w	wall

management perspective, asphaltene deposition has a strong economical impact on the oil industry because it may substantially increase operating costs of oil production and reduce the production rates. Eventually, the production must be curtailed to remove asphaltene deposits from formation, well tubing and surface facilities by wash-out with solvents such as toluene or xylene. These organic chemicals are generally hazardous, expensive and environmentally harmful solvents which may result in high cleaning and downtime costs. Furthermore, considering the trend of the oil industry towards the increased utilization of deeper reservoirs which generally have asphaltenic oil, the role of asphaltene deposition in the economic development of oil discoveries will be important and crucial.

Over the last three decades; extensive research efforts both experimentally and theoretically have been devoted to the understanding of fundamental thermodynamic aspects of asphaltenes in crude oil. The results of these investigations have been summarized in several papers (e.g. Kawanaka et al. [13], Mansoori [14], Deo and Hanson [15], Rahoma et al. [16], Browarzik et al. [17], Monteagudo et al. [18]), books (Chilingarian and Yen [19], Nomura et al. [20], Mullins and Sheu [1], Firoozabadi [21], Becker [22]) and recent Ph.D. theses (e.g. Park [23], Nghiem [24], Alboudwarej [25] and Ashoori [26]) on this subject. It should be emphasized that thermodynamic models alone are not sufficient for solving the problem of asphaltene deposition in the formation, production wells and surface facilities. They only provide information on the solubility of asphaltene in a typical crude oil at specific conditions. Asphaltene deposition is a rate process and the knowledge of the mechanism of deposition and its kinetics are essential to determine how fast the deposition process will take place. Furthermore, the mechanism of the asphaltene deposition can also explain the effect of oil production rate, temperature and flocculated asphaltene concentration on the rate of deposition and the increase of the deposit thickness with time.

A review of the existing literature on mechanisms and kinetics of asphaltene deposition from crude oil reveals that hardly any information is available on this subject. This is mainly because of the difficulty in using the conventional approaches to measure the mass of asphaltene deposition per unit area as a function of time and determine the controlling mechanism and the activation energy of the deposition process. The aim of the present paper is to study the mechanisms and kinetics of asphaltene deposition from asphaltenic crude oils using a thermal approach and to determine the effects of oil velocity, temperature and flocculated asphaltene concentration on the rate of deposition.

2. Background of the measurements

When a clean fluid flows over a hot surface at constant flow rate, bulk temperature and heat flux, the corresponding temperature drop which develops between the hot surface and the bulk of the flowing fluid is shown in Fig. 1a. In this case, the thermal resistance against heat transfer is just the laminar sublayer adjacent to the surface, and the heat transfer coefficient between surface and fluid is defined as:

$$\alpha_0 = \frac{\dot{q}}{T_s^0 - T_b} \tag{1}$$

Eq. (1) shows that as long as flow rate, bulk temperature and heat flux are kept constant and no deposit is formed on the surface,

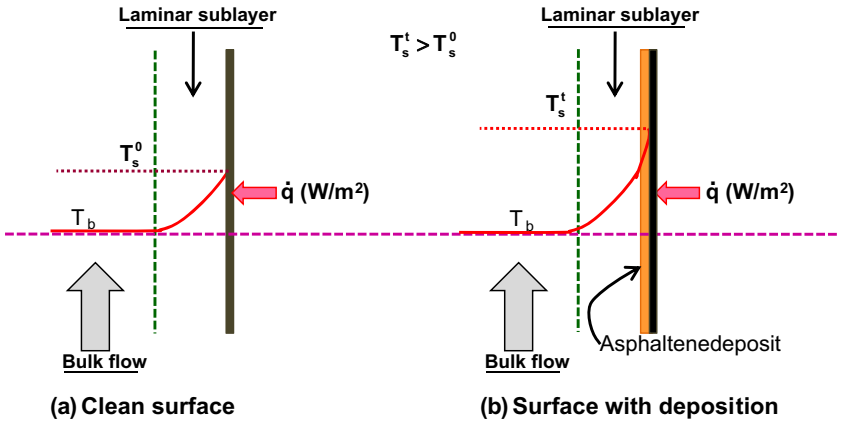

Fig. 1. Temperature profile in the absence and presence of asphaltene deposit.

the heat transfer coefficient α_0 will also remain constant. Asphaltene particles depositing on the surface act as an additional thermal resistance to heat transfer. If the heat flux is maintained constant, the heat transfer coefficient decreases with time and, as a consequence, the surface temperature T_s rises. Thus for a surface with asphaltene deposit we can write (see Fig. 1b):

$$\alpha_t = \frac{\dot{q}}{T_s^t - T_b} \tag{2}$$

The thermal resistance of the formed asphaltene deposit on the surface is equal to (e.g. Jamialahamdi and Müller-Steinhagen [27]):

$$R_A^t = \frac{1}{\alpha_t} - \frac{1}{\alpha_0} \tag{3}$$

The mass of asphaltene deposit per surface area corresponding to this thermal resistance is equal to (e.g. Jamialahmadi and Müller-Steinhagen [28]):

$$m_d^t = \rho_d \lambda_d R_A^t \tag{4}$$

Therefore, if a test rig is designed to measure the variation of surface temperature with time as a result of asphaltene deposition, it allows us to determine the forced convective heat transfer coefficient, the thermal resistance and the corresponding mass of deposit formed on the surface as a function of time, from Eqs. (2)–(4), respectively. Typical values of density and thermal conductivity of the deposit, which have been used in the following calculations, are $\rho_d = 1100$ kg/m^3 and $\lambda_d = 0.75$ W/m K [29].

3. Experimental equipment and procedure

Fig. 2 shows the experimental apparatus which has been used to measure the mass of asphaltene deposition as a function of time via the measurements of the heat transfer coefficient and the thermal resistance of asphaltene deposit. Oil was pumped by a stainless steel pump from a temperature controlled supply tank to the test section via a calibrated orifice plate in conjunction with a pressure transducer. The supply tank can be maintained at a predetermined temperature with an internal cooling coil and three controlled band heaters on the external surface of the tank. The bulk temperature of the oil is measured with K-type thermocouples which are located in the tank and in mixing chambers before and after of test section. The oil flow rate can be controlled with a gate valve prior to the test section in conjunction with the bypass line. The rig is fully insulated to avoid heat losses to the ambient air

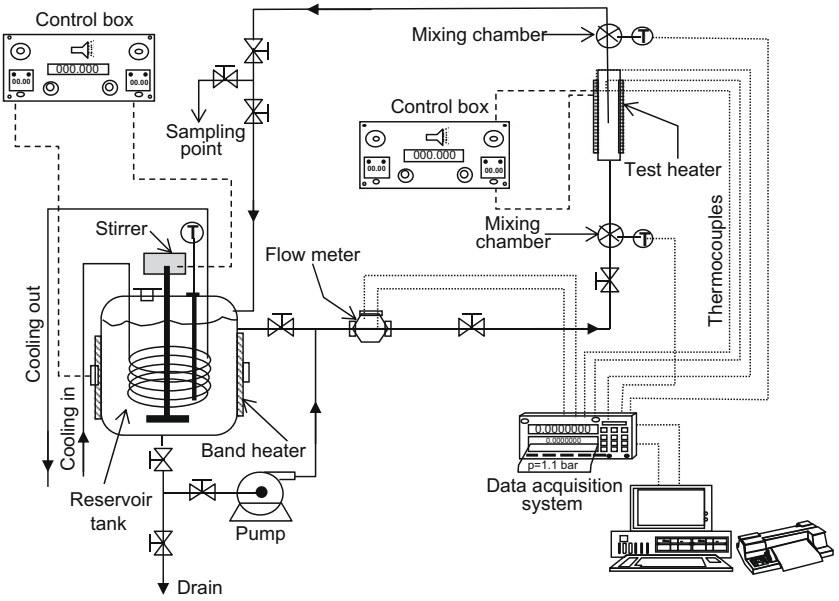

Fig. 2. Schematic drawing of the experimental apparatus.

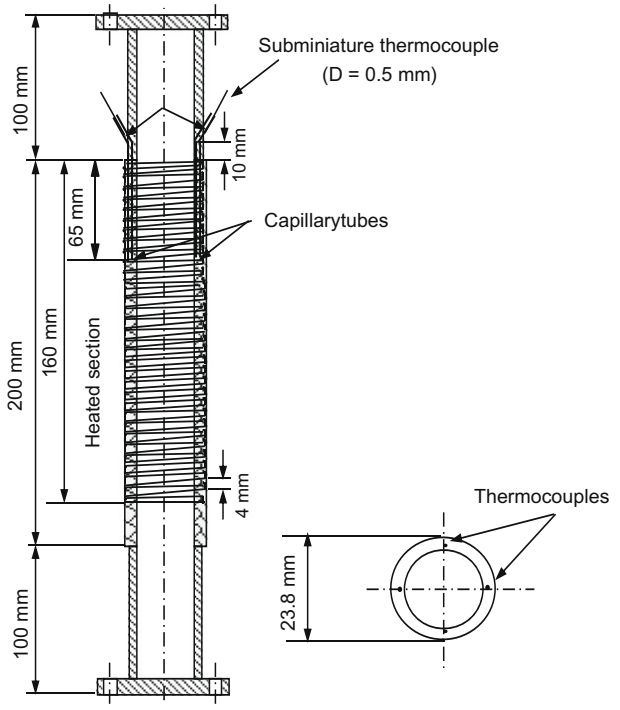

Fig. 3. Schematic diagram of test section.

after the test section. To prevent corrosion all wetted parts of rig and valves are manufactured from stainless steel. Thermocouple voltages, the voltage signals from the flow meter, current and voltage drop from the test heater were all measured and processed with a data acquisition system and adjusted by temperature controllers and variacs. The test section is shown in Fig. 3. It was designed as an externally heated stainless steel pipe. Heat was supplied to the test section by a Thermocoax stainless steel sheathed resistance heater which was fitted into a thread at the pipe outside. To ensure good thermal contact between heater and pipe and an even temperature distribution at the pipe internal surface, the complete arrangement is covered with high temperature silver solder. The important dimensions of the test section are given below:

Inside diameter of pipe	23.8 mm
Heated length	160 mm
Heated length to thermocouple location	95 mm

Four lengths of capillary tubing were soldered into separated external grooves close to the inside surface of the pipe. The local surface temperature of the heated pipe is measured using four miniature E-type thermocouples, which are inserted into these four capillary tubes. The thermocouples are calibrated to measure the temperature at the internal surface of the pipe. This involved determining a correction value to be subtracted from the wall thermocouple temperature, which accounts for the temperature drop due to conduction from the thermocouple location to the internal surface of the tube. The temperature drop between the thermocouple location and the surface can be calculated from:

$$T_s = T_{th} - \dot{q}\frac{s}{\lambda_s} \tag{5}$$

The ratio between the distance of the thermocouples from the surface and the thermal conductivity of the pipe/thermocouple material (s/λ_s) was determined for each thermocouple by careful calibration measurements using a Wilson plot technique. A typical value of s/λ_s was 1.4×10^{-4} m^2 K/W. The local heat transfer coefficient α is calculated from:

$$\alpha = \frac{\dot{q}}{T_s - T_b} \tag{6}$$

Because of the soldering material and the design of the Thermocoax heater, temperatures and heat fluxes for this test section are limited to 200 °C and 150,000 W/m^2, respectively.

3.1. Experimental procedure

Prior to commencing a test run, the test section, reservoir tank and pipes were washed with toluene to remove deposits from the previous experiments. Once the system was cleaned, the crude oil was introduced to the reservoir tank. For deposition experiments, a predetermined volume of normal pentane was also added to the reservoir tank in order to increase the concentration of flocculated asphaltene particles in the oil. Following this, the tank heater was switched on and the temperature of the system allowed to rise. When the temperature of oil in the reservoir tank has reached the desired value, the pump was started and the rig was left to equilibrate to the desired bulk temperature. Meanwhile the velocity of the oil was adjusted to the desired value by the gate valve prior to the test section and a bypass valve to return some oil directly to the reservoir tank. Then, the power was supplied to the test heater and kept at a predetermined value. The data acquisition system was switched on to record temperatures, pressure and heat flux. Samples were taken from the oil during the experiments and analyzed by the gravimetric method (Ashoori [26]). The experiments were carried out at successively lower superficial velocities and some runs were repeated to check the reproducibility of the experiments, which was better than ±5%. The range of the experimental parameters covered in this investigation is shown in Table 1.

3.2. Physical properties of the investigated oil

Forced convective heat transfer and asphaltene deposition experiments were performed using an Iranian asphaltenic crude oil. The fractions of saturates, aromatics, resins and asphaltenes in the oil were obtained from the so-called SARA test and are given in Table 2.

The physical properties of oil under various operating temperature are essential for the calculation of heat transfer coefficients and the mass of asphaltene deposited on the surface. Figs. 4 and 5 present the viscosity, density, specific heat and thermal conductivity of oil versus temperature, respectively [29]. As expected, the

Table 1
Range of operating parameters.

Flow velocity	$0.35 \leqslant v \leqslant 2$ m/s
Heat flux density	$25 \leqslant \dot{q} \leqslant 86$ kW/m^2
Asphaltene supersaturation concentration	0–5 kg/m^3
Bulk temperature	70–85 °C
Surface temperature	100–125 °C

Table 2
SARA test results.

Fractions	Wt%
Saturates	52.49
Aromatics	41.04
Resins	5.48
Asphaltenes	0.99

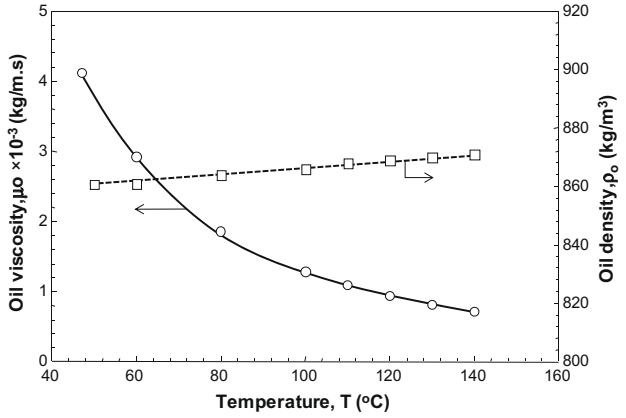

Fig. 4. Variation of oil viscosity and oil density with temperature.

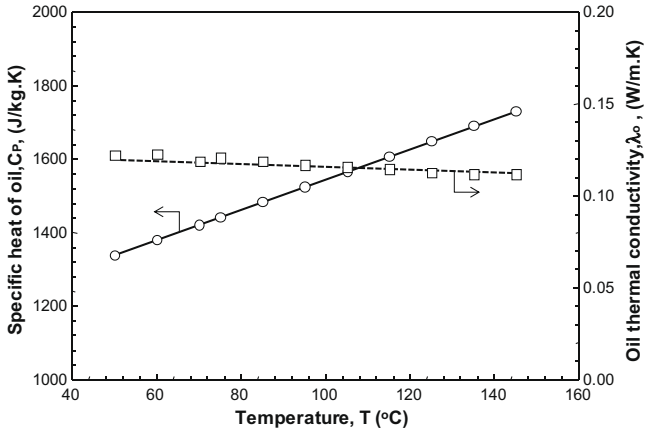

Fig. 5. Variation of specific heat and thermal conductivity of oil with temperature.

viscosity and thermal conductivity of the oil decrease as temperature is increased. Contrariwise, the specific heat increases with oil temperature, while the density remains almost constant.

3.3. Error analysis

The experimental error for the measured mass of asphaltene deposition may be due to errors in the measurement of heat flux, bulk temperature and surface temperature of the test section. As the surface was sanded with grade 240 emery paper, it was postulated that in all experiments the heat transfer was comparable with respect to surface roughness. By repeating several measurements of clean heat transfer coefficients, the same results were obtained, which confirms the above assumption. The error of the adjusted heat flux is due to errors in the measurements of electrical current and voltage. The power delivered by the heater box showed small fluctuations which create a maximum error of about 1.1% of the target value. It is accepted that this phenomenon has some minor effect on the deposition on the test section surface. The temperatures were measured with K-type thermocouples located in the bulk of the oil flow before and after the test section. These thermocouples were initially calibrated against a quartz thermometer with an accuracy of about 0.02 K. The inaccuracy in temperature measurements due to the calibration errors of the thermocouples may lead to a deviation of approximately ±0.2 K. The maximum error in the mass of asphaltene deposition measurements was estimated to be less than ±3.5% by taking into account the temperature, heat flux and flow rate measurement errors.

4. Results and discussion

4.1. Concentration of flocculated asphaltene particles

The determination of the concentration of flocculated asphaltene particles in the oil at specified temperatures is essential to study the mechanisms of asphaltene deposition and to develop a mechanistic deposition model. Fig. 6 shows the measured mass of precipitated asphaltene as a function of the volumetric dilution ratio of normal pentane/oil for several temperatures. The experimental results show that the mass of precipitated asphaltene increases with increasing dilution ratio while it decreases with increasing temperature – which is in agreement with previous findings (e.g. Rassamdama et al. [30], Hu and Guo [31], Ashoori et al. [34]). The fractal aggregation approach is used to correlate these results which have been obtained from the titration of dead oil with normal pentane at different temperatures. Sahimi and coworkers (Rassamdana et al. [7], Dabir et al. [32], Mozaffarian et al. [33], Rassamdana et al. [30]) have shown that all titration curves of asphaltenic dead oil with normal alkane solvents will collapse into a single universal third order polynomial function:

$$Y = A_0 + A_1X + A_2X^2 + A_3X^3 \tag{7}$$

where the constant parameters A_0 to A_3 denote the scaling coefficients. The three main variables of titration of dead oil curves are the weight percentage of precipitated asphaltene W, the solvent to oil dilution ratio R_m and the molecular weight of the solvent. Rassamdana et al. [30] lumped these three parameters into two variables X and Y of the scaling equation (8):

$$X = \frac{R_m}{M^z} \text{ and } Y = \frac{W}{R_m^{z'}} \tag{8}$$

z and z' are two adjustable parameters which must be carefully tuned to obtain the best fit of the experimental data. They suggested $z' = -2$ regardless of oil and precipitant used, and $z = 0.25$. Hu et al. [8] evaluated the universality of exponents z and z' and concluded that z depends on oil composition, varying from 0.2 to 0.5, while z' is effectively universal. In recent years, the validity of the scaling model has been verified by several investigators (e.g. Hu and Guo [31], Ashoori et al. [34], Hong and Watkinson [35]) for titration of dead oils with normal alkane solvents under isothermal conditions. Rassamdana et al. [30] extended the scaling model to non-isothermal asphaltene precipitation processes by including the temperature in the scaling variables X and Y in the following form:

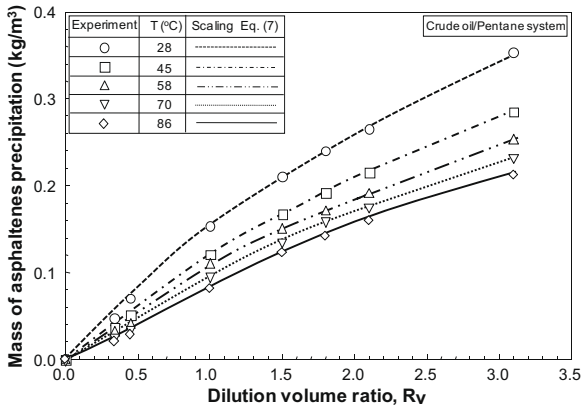

Fig. 6. Variation of mass of asphaltenes precipitation with dilution ratio at various temperatures.

$$X = \frac{R_m}{M^z \cdot T^{c_1}} \quad \text{and} \quad Y = \frac{W}{R^{z'} \cdot X^{c_2}} \tag{9}$$

They reported that the non-isothermal data can be correlated well by setting the exponents c_1 and c_2 equal to 0.25 and 1.6, respectively. Hu and Guo [31] performed extensive titration experiments on dead oil at several temperatures and concluded that the scaling equations (9) are adequate for correlating and predicting the asphaltene precipitation data at different temperatures for normal alkane precipitants, but with exponents z, c_1 and c_2 equal to 0.25, 0.5 and 1.6, respectively. Ashoori et al. [34] slightly modified the scaling equations (9) and retuned them for titration curves of Iranian crude oils with various alkanes:

$$X = \frac{R_v}{M^{0.25}T^{0.4}} \quad \text{and} \quad Y = \frac{W}{(MR_v)^{-0.4}} \tag{10}$$

The applicability of Eqs. (10) for the oil which is used in this investigation is illustrated in Fig. 7 where the plot of Y against X resulted in a single curve. The following third order polynomial is an excellent fit of this curve:

$$Y = 181.38X^3 - 52.997X^2 + 137.31X - 2.201 \tag{11}$$

In this study, Eq. (11) is used to predict the flocculated asphaltene concentration in oil under various operating conditions.

4.2. Clean heat transfer coefficient

Referring to Eq. (3), the second parameter which is needed for the calculation of the mass of deposited asphaltene is the clean forced convective heat transfer coefficient α_0 to the flowing oil. A review of the existing literature on this subject reveals no detailed information on forced convective heat transfer to crude oil. There is a lack of published experimental data and the exact effects of operating variables such as oil velocity on forced convective heat transfer coefficients to oil are still uncertain. Knowledge of convective heat transfer to oil is also needed for accurate prediction of well and well-tubing surface temperatures to solve production engineering problems. Due to the importance of well temperature, several different models have been developed for calculation of well temperature gradients over the years (e.g. Ramey [36], Green and Whillhite [37], Takacs [38]). These models recommended the McAdams [39] correlation for the calculation of forced convective heat transfer coefficients to crude oil. This correlation is rather old and its application for crude oil has not been verified yet. Forced convective heat transfer coefficients are measured for different heat fluxes over a range of oil velocities from 0.35 m/s to 2.5 m/s. With increasing oil velocity, the fluid turbulence is intensified and the heat transfer coefficient is improved as the boundary layer gets thinner.

A considerable number of correlations exist for the prediction of turbulent heat transfer coefficients in pipes. For fully developed turbulent flow in pipes, Nusselt numbers are in most cases correlated by the following general functionality which has been obtained from dimensional analysis:

$$Nu = kRe^a Pr^b \tag{12}$$

A number of such correlations are listed in Table 3. The values of the parameter k, and the exponents a and b vary according to the experimental data on which the correlations have been developed.

Prandtl [44] developed Eq. (13) for fully developed turbulent flow in pipes:

$$Nu = \frac{\frac{f}{8}Re \cdot Pr}{k_1 + k_2\sqrt{\frac{f}{8}}(Pr^n - 1)} \tag{13}$$

Prandtl suggested that $k_1 = 1$, $k_2 = 8.7$ and $n = 1$. Petukhov and Popov [45] modified these values to $k_1 = 1$, $k_2 = 12.7$ and $n = 2/3$. Eq. (13) is based on a model for fully developed turbulent flow, but it does not account for entrance effects. To overcome this deficiency, Gnielinski [46] modified Eq. (13) by replacing Re by $(Re - 1000)$ and by multiplying it with an entrance correction factor derived by Hausen [47]. This resulted in:

$$Nu = \frac{\frac{f}{8}(Re - 1000)Pr}{1 + 12.7\sqrt{\frac{f}{8}}\left(Pr^{\frac{2}{3}} - 1\right)}\left[1 + \frac{1}{3}\left(\frac{D}{L}\right)^{\frac{2}{3}}\right]\left(\frac{Pr_b}{Pr_w}\right)^{0.11} \tag{14}$$

For Eq. (14), the friction factor for turbulent flow in technically smooth pipes is to be calculated according to Filonenko [48]:

$$f = (1.821\log_{10}Re - 1.64)^{-2} \tag{15}$$

To put the accuracy of these correlations into perspective, their predictions are compared with experimental data in Fig. 8. While all

Table 3
Published correlations for forced convective heat transfer.

Authors	Correlations
Dittus and Boelter [40]	$Nu = 0.023Re^{0.8}Pr^{0.3}$
McAdams [39]	$Nu = 0.023Re^{0.8}Pr^{0.4}$
Berger and Hau [41]	$Nu = 0.0167Re^{0.875}Pr^{\frac{1}{3}}$
Whitaker [42]	$Nu = 0.015Re^{0.83}Pr^{0.42}$
Kays and Crawford [43]	$Nu = 5 + 0.015Re^aPr^b$ where a and b are given as : $a = 0.88 - \frac{0.24}{4+Pr}$, $b = 0.333 + 0.5\exp(-0.6Pr)$

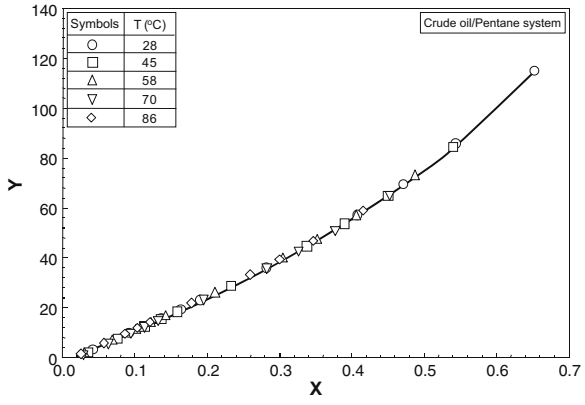

Fig. 7. Correlation of scaling parameters, showing that asphaltene precipitation data are collapsing onto a single curve.

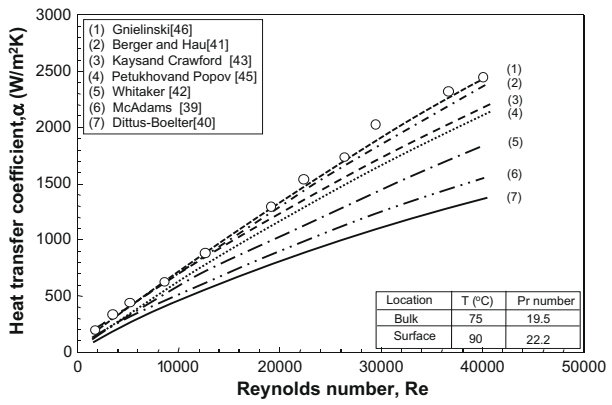

Fig. 8. Comparison of measured forced convective heat transfer coefficients to oil with the prediction of published correlastions.

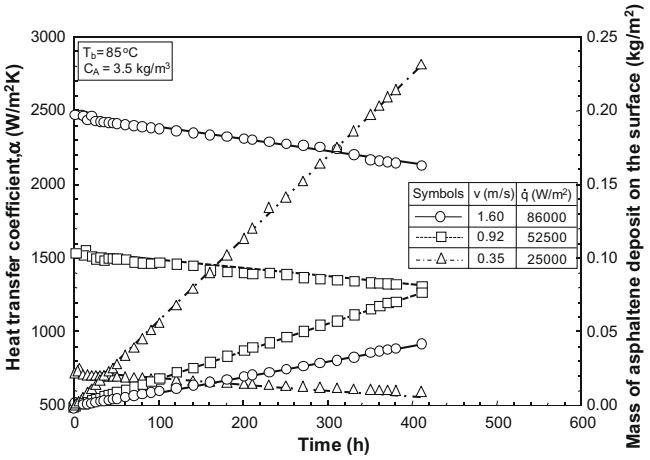

Fig. 9. Typhical variation of heat transfer coefficients and corresponding mass of asphaltene deposition with time for various heat fluxes and oil velocities.

correlations predict a considerable increase in heat transfer coefficient with increasing oil Reynolds number, the variation between the predictions of the various correlations is quite considerable. The Gnielinski [46] and the Berger and Hau [41] correlations fit the experimental results for forced convective heat transfer to crude oil better than the other correlations. The disagreement between experimental results and predicted values from the correlations of McAdams [39] and Dittus and Boelter [40] is significant.

4.3. Asphaltene deposition experiments

Fig. 9 shows heat transfer coefficients and the corresponding mass of asphaltene deposit as a function of time for heat fluxes ranging from 25,000 to 86,000 W/m^2, flocculated asphaltene concentration of 3.5 kg/m^3, oil velocity varying from 0.35 to 1.56 m/s and a bulk temperature of 85 °C. The deposit layer of asphaltene formed on the surface acts as an additional resistance which is the reason for the reduction of heat transfer coefficient. The general shape of the heat transfer coefficient versus time curves is remarkably concordant. It is characterized by slight fluctuations of the heat transfer coefficient at the very beginning of the operating time, followed by a gradual decrease. The initial fluctuations are a result of the adjustment of heat flux and the increased roughness of the surface due to the initial asphaltene deposits. The rough surface increases the turbulence level in the flow zone near the heat transfer surface and, therefore, may temporarily improve the heat transfer coefficient until the insulating effect of the growing asphaltene deposit becomes dominant. There is usually a time interval between the start of the experiment and the detection of a thermal resistance due to the deposition process. This is called the delay time or initiation period. During this period, certain conditions required for deposition such as adsorption of asphaltene particles to the surface and surface conditioning are established. The results show that the heat transfer coefficients at high heat fluxes decrease faster and to a larger extent than at low heat fluxes. The thermal resistance of the asphaltene deposit layer can be calculated from the initial heat transfer coefficient when the surface is still clean and the actual heat transfer coefficients, according to Eq. (3). The clean heat transfer coefficient α_0 is calculated from the Gnielinski [46] correlation. The mass of asphaltene deposit per unit area can be obtained as a function of time by substituting Eq. (3) into Eq. (4):

$$m_d = \rho_d \lambda_d \left(\frac{1}{\alpha_t} - \frac{1}{\alpha_0} \right) \tag{16}$$

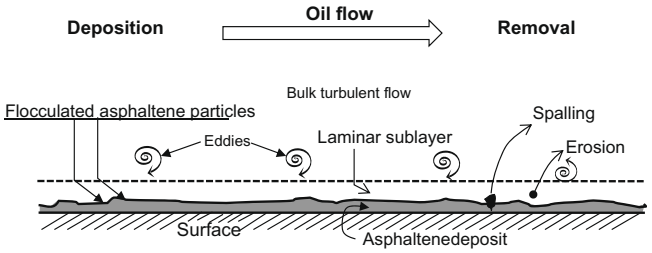

Fig. 10. Schematic representation of asphaltene deposition and removal.

Generally, three basic stages may be visualized in relation to deposition on a surface from a moving fluid. Referring to Fig. 10, they are:

1. The diffusional transport of the particles across the boundary layers adjacent to the surface.
2. The adhesion of the deposit matter to the metal surface and to itself.
3. The removal of patches of deposited asphaltene particles from the surface and their transport away from the surface.

The sum of these basic mechanisms represents the growth rate of the asphaltene on the surface. In mathematical terms the net rate of growth of asphaltene deposit may be regarded as the difference between the rates of deposition and removal of flocculated asphaltene particles from the surface. In more precise mathematical terms it can be presented as (Kern and Seaton [49]):

$$\frac{dm}{dt} = \dot{m}_d - \dot{m}_r \tag{17}$$

Eq. (17) shows that the asphaltene deposition is a dynamic process and that it changes with time in a manner determined by the rates of deposition and removal. Eq. (17) can be represented as a net mass of deposit versus time curve. If the deposit is adherent, the removal rate of deposited asphaltene particles can be ignored and the rate of deposition increases linearly with time. Asymptotic deposition is generally characteristic of soft and weakly adherent deposits, which flake off easily due to the shear force of the fluid flowing past them. This behavior can be obtained if the deposition rate is constant and the removal rate is proportional to the thickness of the deposit. The falling rate behavior may result from a falling deposition rate or from a constant deposition rate and an increasing removal rate. The experimental results of the present investigation show a more or less linear increase in the fouling resistance with time, for the range of investigated oil velocities. This indicates that during the first few weeks of the deposition process when the thickness of asphaltene deposit on the surface is small, no significant removal from the surface takes place and the rate of deposition remains almost constant. This may be the reason why asphaltene deposits in production wells and surface facilities frequently plug the flow channels, particularly at low velocities. However, it may be postulated that after a long time, when a substantial thickness of deposit on the surface is reached, some deposit may come off by the mechanism of shear-related erosion or removal. Oil velocity, flocculated asphaltene concentration and surface temperature were found to be the three major parameters affecting the rate of deposition.

4.4. Effect of oil velocity

Many studies have attempted to clarify the effect of flow velocity on the deposition process. High velocities can sometimes reduce deposition (e.g. Hasson and Zahavi [50]), in other instances (e.g. Hatch [51]) an increase in deposition has been reported. As

discussed in several reference books (e.g. [52]), if the deposition process is not mass transfer controlled, then the deposition rate should be independent of the flow velocity as long as the surface and bulk temperatures remain constant. To identify the controlling mechanism, the asphaltene deposition rate was determined over a wide range of oil velocities under constant concentration, bulk and initial surface temperatures. The results of these measurements are summarized in Fig. 11. The deposition rates which are obtained from the slope of these curves are plotted as a function of oil Reynolds number in Fig. 12. The rate of deposition decreases significantly as oil velocity is increased. Assuming that there is insignificant deposit erosion (see previous section) this can only mean that the sticking probability of particles reaching the surface must decrease with increasing flow velocity. This hypothesis was already discussed in detail for particulate fouling by Epstein [53]. In particulate processes, the rate of deposition decreases with fluid velocity as given in Eq. (18):

$$\dot{m}_d \propto \frac{1}{v^j} \tag{18}$$

Depending on the controlling mechanism, reported values of j lie in the range of 0.35–2. The present results indicate that the deposition rate of flocculated asphaltene particles on the surface is almost inversely proportional to the oil velocity, i.e. j is approximately equal to one.

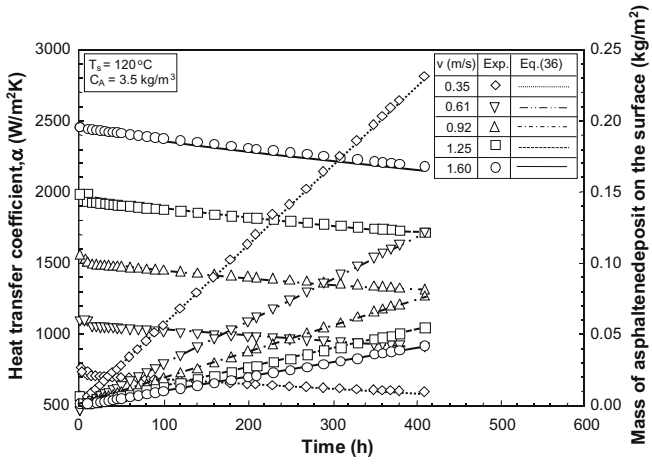

Fig. 11. Heat transfer coefficients and corresponding mass of asphaltene deposit as a function of time showing the effect of oil velocity.

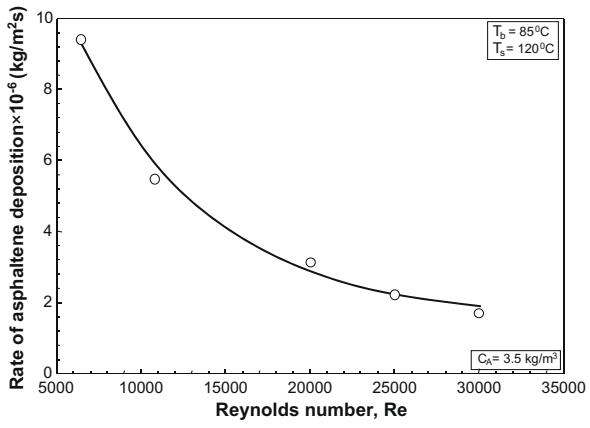

Fig. 12. Variation of asphaltene deposition rate with oil Reynolds numbers.

4.5. Effect of flocculated asphaltene concentration

The primary cause of asphaltene deposition is the concentration of flocculated asphaltene in the flowing oil. As long as the removal rate can be ignored and all particles arriving at the heat transfer surface stick to it, the rate of deposition may be generally expressed as:

$$\dot{m}_d = k(C_{As})^n \tag{19}$$

where C_{As} is the flocculated asphaltene concentration at the surface conditions. For mass transfer and surface deposition controlled processes n generally varies between 1 and 2. Eq. (19) shows that regardless of the mechanism of deposition the effect of concentration is strong. The observed effect of flocculated asphaltene concentration at a velocity of 1.25 m/s and constant bulk and initial surface temperature is shown in Fig. 13. The results indicate that the decline of heat transfer coefficient and the rate of asphaltene deposition both increase as the concentration of flocculated asphaltene is increased.

4.6. Effect of surface temperature

Fig. 14 shows a typical variation of heat transfer coefficients and the corresponding mass of asphaltene deposit for different surface

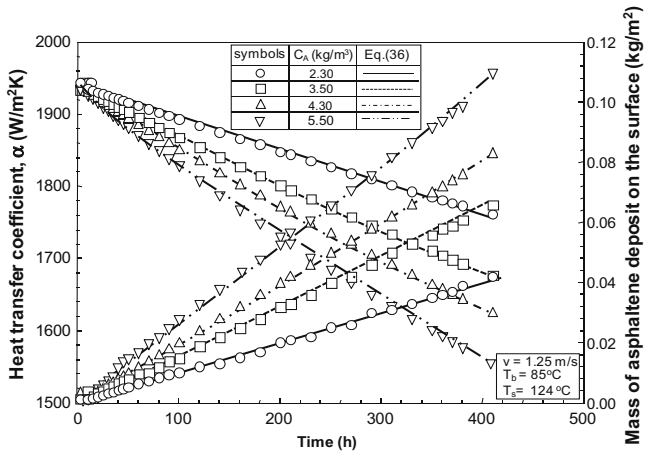

Fig. 13. Heat transfer coefficients and mass of asphaltene deposit as a function of time showing the effect of flocculated asphaltene concentration.

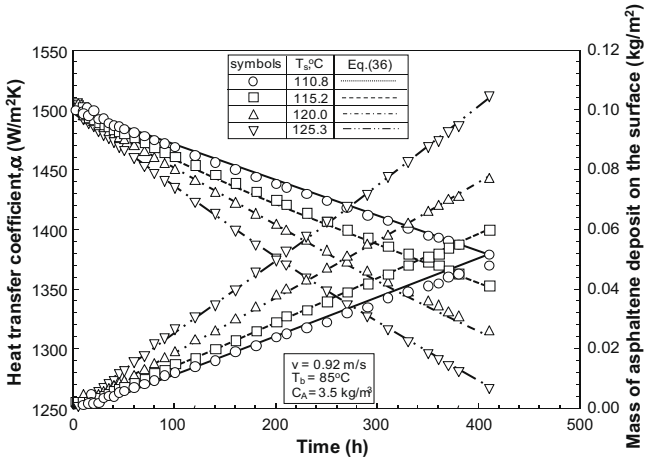

Fig. 14. Heat transfer coefficients and mass of asphaltene deposit as a function of time showing the effect of surface temperature.

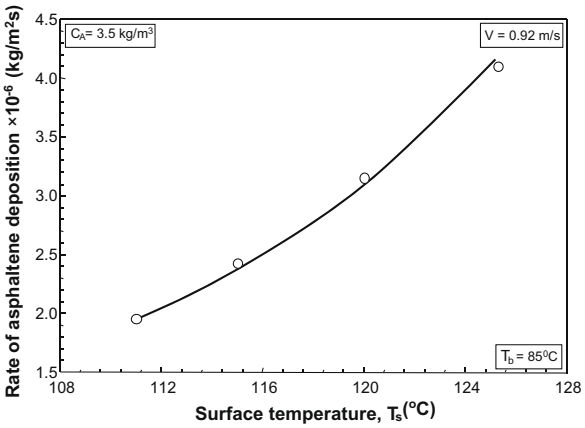

Fig. 15. Variation of asphaltene deposition rate with surface tempereture.

temperatures, at constant bulk temperature, oil velocity and asphaltene concentration. The heat transfer coefficient decreases faster at higher temperature and, therefore, the rate of asphaltene deposition must increase as the surface temperature is raised. The effect of surface temperature on the rate of asphaltene deposition is shown in Fig. 15. These results indicate that the rate of deposition of asphaltene particles on the surface depends strongly on the surface temperature. The main effect of surface temperature on the rate of asphaltene deposition on the surface is through the diffusivity of asphaltene particles and the attachment rate constant of the process. As will be shown in the following chapter, mass transfer coefficients are a linear function of temperature while the attachment rate constants generally increase exponentially with surface temperature according to an Arrhenius relationship. The non-linear trend shown in Fig. 15 may indicate that both mechanisms are important with respect to the overall rate of deposition.

5. Mechanisms of deposition

Two processes must occur before an asphaltene particle originally suspended in the oil flow becomes part of the deposit layer. First the particle has to be transported to the surface by one or a combination of mechanisms including Brownian motion, turbulent diffusion or by virtue of the momentum possessed by the particle. The size of the particle will have a large influence on the dominant mechanism. For instance very small particles are predominantly subject to Brownian and eddy diffusion, whereas large particles because of their mass will move under momentum forces. Having arrived at the surface the asphaltene particle must stick to become part of the deposit layer residing on the surface.

5.1. Deposition process

In the first step of the deposition process, particles are transported to the surface by diffusion through the boundary layer which is formed between the surface and the oil:

$$\dot{m}_d = k_t(C_{Ab} - C_{As}) \tag{20}$$

where k_t is a transport coefficient. In the case of ions, molecules and submicron asphaltene particles, the transport is diffusional in nature and k_t is equivalent to the well known mass transfer coefficient, β, which can be obtained from published correlations for forced convective mass transfer, provided that the diffusivity of the asphaltene particles can be determined. For submicron particles, the Brownian diffusion coefficient can be determined from the Stokes–Einstein equation (Bott [54]):

$$D_{Diff} = \frac{k_B T}{3\pi\mu d_p} \tag{21}$$

Determination of asphaltene particle size distribution has been discussed in detail by Ashoori [26]. For asphaltene particles of 0.5 μm diameter suspended in oil, which is a reasonable value for the present investigation, Eq. (21) predicts diffusion coefficients in the order of 10^{-12} m^2/s and Schmidt numbers in the order of 10^6. The mass transfer coefficient for turbulent flow can be calculated from the Prandtl equation (13) and the Chilton and Colburn analogy by replacing the Nusselt and Prandtl numbers by the Sherwood and Schmidt numbers, respectively. Eq. (13) then reads:

$$Sh = \frac{\frac{f}{8} Re \cdot Sc}{1 + 12.7\sqrt{\frac{f}{8}}\left(Sc^{\frac{2}{3}} - 1\right)} \tag{22}$$

For asphaltene particles with Schmidt numbers in the order of 10^6, after some mathematical manipulations, Eq. (22) simplifies to:

$$\beta = \frac{0.079\sqrt{\frac{f}{8}} \cdot v}{Sc^{\frac{2}{3}}} \tag{23}$$

It is interesting to note that Cleaver and Yates [55] used an entirely different approach based on a computation of the stagnation flow towards the wall to derive the following expression for the diffusion regime of particle deposition:

$$\beta = \frac{0.084\sqrt{\frac{f}{8}} \cdot v}{Sc^{\frac{2}{3}}} \tag{24}$$

Epstein [53] used the Reichardt [56] analogy and derived Eq. (25) for mass transfer coefficients for turbulent flow with high Schmidt numbers:

$$\beta = \frac{0.0847\sqrt{\frac{f}{8}} \cdot v}{Sc^{\frac{2}{3}}} \tag{25}$$

It is noteworthy to realize that excellent agreement exists between Eqs. (23)–(25), despite the different ways they have been derived. These correlations indicate that:

$$\beta \propto d_p^{-\frac{2}{3}} \cdot v \tag{26}$$

For a constant average particle size, Eq. (26) may be simplified to:

$$\beta = k_1 v \tag{27}$$

Substituting Eq. (27) into Eq. (20) results in:

$$\dot{m}_d = k_1 v(C_{Ab} - C_{As}) \tag{28}$$

Eq. (28) shows that the rate of mass transfer of asphaltene particles from the bulk flow of oil to the surface is proportional to the oil velocity. In the above equations (with the exception of Eq. (14)), the Fanning friction factor, f, can be calculated from the classical Blasius equation for smooth tube flow:

$$f = \frac{0.3164}{Re^{0.25}} \tag{29}$$

5.2. Attachment process

Attachment of the asphaltene particles to the surface takes places after mass transfer of the asphaltene particles from the bulk of the oil flow to the surface. While, in theory, fluid mechanics and diffusion theory can explain how asphaltene particles get to the surface, it is not possible to predict whether or not a particle subsequently will adhere to the surface. The problem of attachment can be formulated statistically in terms of the probability that a

particle which arrives at the surface sticks to it, or alternatively the fraction of particles reaching the wall which stay there. The general correlation approach is then to replace the driving concentration difference in Eq. (28) by the product of bulk concentration and sticking probability. Thus:

$$\dot{m}_d = S_P \beta C_{Ab} \tag{30}$$

Therefore, for $S_P = 1$, mass transfer controls and, according to Eq. (28), $\dot{m}_d$ is directly proportional to the oil velocity. For $S_P < 1$, surface attachment is important and $\dot{m}_d$ may decrease as the oil velocity increases. Asphaltene particles adhere to the surface if the physico-chemical adhesive forces between the asphaltene particles and the surface overcome the drag forces exerted near the surface (Watkinson and Epstein [57]):

$$S_P = S_0 \frac{F_{adh}}{F_{drag}} \tag{31}$$

where S_0 is some appropriate constant. The adhesion forces generally obey an Arrhenius-type expression and may be written as:

$$F_{adh} = F_a e^{-\frac{E_a}{RT_s}} \tag{32}$$

where F_a is constant, E_a is the activation energy of adhesion and T_s is the surface temperature. On the other hand, the drag force depends on drag coefficient, cross-section of the asphaltene particles in the flow direction, oil density and velocity:

$$F_{drag} = C_D A_P \rho v^2 \tag{33}$$

Therefore, by substituting Eqs. (32) and (33) into Eq. (31), sticking probability, S_P, may be written as:

$$S_P = k_2 \frac{e^{-\frac{E_a}{RT}}}{v^2} \tag{34}$$

Substituting Eq. (34) into Eq. (30) yields:

$$\dot{m}_d = \frac{k_d \beta}{v^2} e^{-\frac{E_a}{RT_s}} \cdot C_{Ab} \tag{35}$$

Here E_a and k_d were found curve-fitting of the experimental data as 65.3 kJ/mole and 9.76×10^8 m^2/s^2, respectively. The mass transfer coefficient β is calculated from either Eqs. (23)–(25) if the Schmidt Number is known.

Eq. (35) may be further simplified by substitution for the mass transfer coefficient β from Eq. (27) and rearrangement of results:

$$\dot{m}_d = \frac{k'_d}{v} e^{-\frac{E_a}{RT_s}} C_{Ab} \tag{36}$$

Eq. (36) shows that the rate of attachment of flocculated asphaltene particles in oil to the surface is proportional to the concentration and inversely proportional to the oil velocity, which is in good agreement with the present experimental observations. The deposition coefficient k_d has been obtained by curve-fitting the present data as 1.55×10^2 m^2/s^2, but will vary with origin of crude oil. Using these fitted values, predictions of Eq. (36) have also been included in Figs. 11, 13 and 14. The calculated trends are in good agreement with the experimental data. This equation predicts all experimental data for the investigated range of operating conditions with an absolute average error of 7.5%.

6. Conclusions

From the perspective of oil reservoir management, understanding the mechanisms and determining the rate of asphaltene deposition across the production wells has a high priority. Asphaltene deposition on well-tubing surface reduces the production of oil considerably. The present study shows that oil velocity, bulk and surface temperature, and flocculated asphaltene concentration have the main influence on the deposition process. The deposition rate is increased as flocculated asphaltene concentration and surface temperature are increased. The deposition rate is inversely proportional to the oil velocity and decreases as the oil velocity is increased. The experimental results have been used to develop a mechanistic model for the prediction of the rate of asphaltene deposition. Considering the complexity of the deposition process, the quantitative agreement between measured and predicted values is good.

References

[1] O. Mullins, E.Y. Sheu, Structures and Dynamics of Asphaltenes, first ed., Springer, London, 1999.
[2] T.F. Yen, J.G. Erdman, S.S. Pollack, Investigation of the structure of petroleum asphaltenes by X-ray diffraction, Anal. Chem. 33 (1961) 1587–1594.
[3] J.G. Speight, The structure of petroleum asphaltenes: current concept. Information Series 81, Alberta Research Council, Edmonton, 1978.
[4] T.F. Yen, The nature of asphaltenes in heavy oil, in: Pan Pacific Synfuels Conference, vol. 2, 1982, pp. 547–557.
[5] NE. Burke, R.D. Hobbs, S.F. Kashou, Measurement and modeling of asphaltene precipitation from live reservoir system, SPE Paper No. 18273, 1990.
[6] S.I. Andersen, Flocculation onset titration of petroleum asphaltenes, Energy Fuels 13 (1999) 315–322.
[7] H. Rassamdana, B. Dabir, M. Nematy, M. Farahani, M. Sahimi, Asphalt flocculation and deposition: 1. The onset of precipitation, AIChE J. 42 (1996) 10–22.
[8] Y.F. Hu, G.J. Chen, J.T. Yang, T.M. Guo, A study on the application of scale equations for asphaltene precipitation, Fluid Phase Equilibr. 171 (2000) 181–195.
[9] D. Vazquez, G.A. Mansoori, Identification and measurement of petroleum precipitates, J. Petrol. Sci. Eng. 26 (1999) 49–55.
[10] S.L. Kokal, J. Najman, S.G. Sayegh, A.E. George, Electro-kinetic and adsorption properties of asphaltenes. Petroleum recovery, J. Can. Petrol. Technol. 31 (1992) 24–30.
[11] C.S. Kabir, A.K.M. Jamaluddin, Asphaltene characterization and mitigation in South Kuwait's Marrat Reservoir, SPE Prod. Facil. (2002) 251–257.
[12] S.L. Kokal, A. Al-Ghamdi, D. Krinis, Asphaltene precipitation in high gas/oil ratio wells, SPE 81567 (2003).
[13] S. Kawanaka, S.J. Park, A. Mansoori, The role of asphaltene deposition in EOR gas flooding, SPE 17376 (1988).
[14] A. Mansoori, Modeling of asphaltene and other heavy organic deposits, J. Petrol. Sci. Eng. 17 (1997) 101–111.
[15] M.D. Deo, U. Hanson, Asphaltene precipitation: a need for a broader view, SPE 25193 (1993).
[16] S.M. Rahoma, L. Watson, A.C.S. Ramos, C.C. Degado, V.R. Almeida, Reversibility and inhibition of asphaltene precipitation in Brazilian crude oils, Petrol. Sci. Technol. 17 (1999) 877–896.
[17] D. Browarzik, H. Laux, I. Rahimian, Asphaltene flocculation in crude oil systems, Fluid Phase Equilibr. 154 (1999) 285–300.
[18] J.E.P. Monteagudo, P.L.C. Lage, K. Rajagopal, Towards a polydisperse molecular thermodynamic model fro asphaltene precipitation in live-oil, Fluid Phase Equilibr. 187–188 (2001) 443–471.
[19] G.V. Chilingarian, T.F. Yen, Asphaltenes and Asphalts, first ed., Elsevier, New York, 2005.
[20] M. Nomura, P.M. Rahimi, O.R. Koseoglu, Heavy Hydrocarbon Resources: Characterization, Upgrading, and Utilization, first ed., Oxford University Press, Oxford, UK, 2005.
[21] A. Firoozabadi, Thermodynamics of Hydrocarbon Reservoirs, McGraw-Hill, New York, 1999.
[22] J.R. Becker, Crude Oil Waxes, Emulsions and asphaltenes, first ed., Pennwell Books, New York, 1997.
[23] S.J. Park, A thermodynamic polydisperse polymer model: application in asphaltene deposition, Ph.D. thesis, University of Illinois at Chicago, Chicago, Illinois, 1989.
[24] L.X. Nghiem, Phase behavior modeling and compositional simulation of asphaltene deposition in reservoirs, Ph.D. thesis, Department of Civil and Environmental Engineering, Edmonton, Alberta, 1999.
[25] H. Alboudwarej, Asphaltene deposition in flowing systems, Ph.D. thesis, University of Calgary, Calgary, Alberta, Canada, 2003.
[26] S. Ashoori, Mechanism of asphaltene deposition in porous media, Ph.D. thesis, Department of Chemical and Process Engineering, University of Surrey, Guildford, UK, 2005.
[27] M. Jamialahmadi, H. Müller-Steinhagen, Reduction of calcium sulfate deposition during nucleate boiling by addition of EDTA, Heat Transfer Eng. J. 12 (1991) 19–26.
[28] M. Jamialahmadi, H. Müller-Steinhagen, Heat exchanger fouling and cleaning in the dihydrate process for the production of phosphoric acid, IChemE J. 85 (A2) (2007) 1–11.
[29] PVT of reservoir fluid and asphaltene experiment, NIOC Confidential Report No. 5265, August, 2005.

[30] M. Rassamdana, M. Farhani, B. Dabir, M. Mozaffarian, M. Sahimi, Asphalt flocculation and deposition: V. The effect of temperature, pressure, and composition, Fuel 13 (1999) 176–187.
[31] Y.F. Hu, T.M. Guo, Effect of temperature and molecular weight of *n*-alkane precipitants on asphaltene precipitation, Fluid Phase Equilibr. 192 (2001) 13–25.
[32] B. Dabir, M. Nematy, A.R. Mehrabi, H. Rassamdana, M. Sahimi, Asphalt flocculation and deposition: III. The molecular weight distribution, Fuel 75 (1996) 1633–1645.
[33] B. Mozaffarian, B. Dabir, M. Sohrabi, H. Rassamdana, M. Sahimi, Asphalt flocculation and deposition: IV. Dynamic evolution of heavy organic compounds, Fuel 76 (1997) 1479–1490.
[34] S. Ashoori, M. Jamialahmadi, H. Müller-Steinhagen, K. Ahmadi, A new scaling equation for modeling of asphaltene precipitation, SPE 85673 (2003).
[35] E. Hong, P. Watkinson, A study of asphaltene solubility and precipitation, Fuel 83 (2004) 1881–1887.
[36] H.J. Ramey, Well heat transmission, J. Petrol. Technol. (1962) 427–440.
[37] D.W. Green, G.P. Willhite, Enhanced oil recovery, Henry L. Doherty Memorial Fund of AIME Society of Petroleum Engineers, Richardson, TX, USA, 2003.
[38] G. Takacs, Gas Lift Manual, Pennwell Corporation, USA, 2005.
[39] W.H. McAdams, Heat Transmission, third ed., McGraw-Hill Book Co., Inc., New York, 1954.
[40] F.W. Dittus, L.M.K. Boelter, Heat Transfer in Automobile Radiators of Tubular Type, University of California Press, Berkeley, CA, 1930. pp. 13–18.
[41] F.P. Berger, K.F. Hau, Mass transfer in turbulent pipe flow measured by the electrochemical method, Int. J. Heat Mass Transfer 20 (11) (1977) 1185–1194.
[42] S. Whitaker, Forced convective heat transfer correlations for flow in pipes past flat plates, single cylinders, single sphere, and for flow in packed beds and tube bundles, AIChE J. 18 (1972) 361–371.
[43] W.M. Kays, M.E. Crawford, Convective Heat and Mass Transfer, McGraw-Hill Book Co., Inc., New York, 1980.
[44] L. Prandtl, Führer durch die Strömungslehre, Verlag Vieweg, Braunschweig, 1944.
[45] B.S. Petukhov, V.N. Popov, Theoretical calculation of heat exchanger and frictional resistance in turbulent flow in tubes of an incompressible fluid with variable physical properties, High Temp. (USSR) 1 (1963) 69–83.
[46] V. Gnielinski, Wärmeübertragung in Rohren, VDI-Wämeatlas, sixth ed., VDI-Verlag, Düsseldorf, 2002.
[47] H. Hausen, Darstellung des Wärmeüberganges in Rohren durch verallgemeinerte Potenzbeziehungen, Z. Ver. Deutsch. Ing. Beiheft Verfahrenstechnik. (4) (1943) 91–134.
[48] G.K. Filonenko, Hydraulic resistance in pipes, Teploenergetika 1 (1954) 40–44.
[49] D.O. Kern, R.E. Seaton, A theoretical analysis of thermal surface fouling, Brit. Chem. Eng. 14 (5) (1959) 258–263.
[50] D. Hasson, J. Zahavi, Mechanism of calcium sulfate scale deposition on heat transfer surfaces, Ind. Eng. Chem. Fund. 9 (1970) 1–10.
[51] G.B. Hatch, Evaluation of scale tendencies, Mater. Prot. Perform. (1973) 49–55.
[52] H. Müller-Steinhagen, Heat Exchanger Fouling – Mitigation and Cleaning Technologies. PUBLICO Publications, 2000. ISBN 3-934736-00-9.
[53] N. Epstein, Particulate Fouling of Heat Transfer Surfaces: Mechanisms and Models, Fouling Science and Technology, Kluwer Academic Publisher, 1988. pp. 143–164.
[54] T.R. Bott, Fouling of Heat Exchangers, Elsevier Publishing Corporation, Amsterdam, The Netherlands, 1995. pp. 62–64.
[55] J.W. Cleaver, B. Yates, The effect of re-entrainment on particle deposition, Chem. Eng. Sci. 31 (1976) 147–151.
[56] H. Reichardt, Fundamentals of turbulent heat transfer, translated from Arch. Ges. Wärmetech. No. 6/7, NACA TM 1408, 1957 and N-41947, 1956.
[57] P. Watkinson, N. Epstein, Particulate fouling of sensible heat exchangers, in: Presented at the Fourth International Heat Transfer Conference, Versailles, France, 1970.